Supplementary Text

Table – S1: Equations governing the dynamics of Module-1

$C_m \frac{dV}{dt} = -\left(I_K + I_{Ca} + I_{K(Ca)} + I_{K(ATP)}\right)$	S11
$\frac{dn}{dt} = \frac{[n_\infty(V) - n]}{\tau_n}$	S12
$\frac{dCa}{dt} = f_{cyt}(J_{mem} + J_{er})$	S13
$\frac{dCaer}{dt} = f_{er}\sigma_v J_{er}$	S14
$\frac{dADP}{dt} = \frac{\left(ATP - ADPexp\left[(r+\gamma)\left(1 - \frac{Ca}{r_1}\right)\right]\right)}{\tau_a}$	S15
$\frac{dG6P}{dt} = \lambda(R_{GK} - R_{PFK})$	S16
$\frac{dFBP}{dt} = \lambda\left(R_{PFK} - \frac{1}{2}R_{GPDH}\right)$	S17

Table – S2: Description of the different terms involved in the differential equations governing the dynamics of Module-1

$I_K = \overline{g_K} n(V - V_K)$	S18
$I_{Ca} = \overline{g_{Ca}} m_\infty(V)(V - V_{Ca})$	S19
$O_\infty(ADP, ATP) = \frac{0.08\left(1 + \frac{2MgADP^-}{17\mu M}\right) + 0.89\left(\frac{MgADP^-}{17\mu M}\right)^2}{\left(1 + \frac{MgADP^-}{17\mu M}\right)^2\left(1 + \frac{ADP^{3-}}{26\mu M} + \frac{ATP^{4-}}{1\mu M}\right)}$	S20
$ADP^{3-} = 0.135ADP$ ATP^{4-}=0.05ATP	S21
$MgADP^- = 0.165ADP$	S22
$g_{K(Ca)} = \overline{g_{K(Ca)}}\left(\frac{Ca^2}{K_D{}^2 + Ca^2}\right)$	S23

$\mathbf{g}_{K(ATP)} = \overline{g_{K(ATP)}} O_{\infty}(ADP, ATP)$	S24
$\mathbf{I}_{K(Ca)} = g_{K(Ca)}(V - V_K)$	S25
$\mathbf{I}_{K(ATP)} = g_{K(ATP)}(V - V_K)$	S26
$\mathbf{n}_{\infty}(V) = \frac{1}{1 + e^{\frac{-(16+V)}{5}}}$	S27
$\mathbf{m}_{\infty} = \frac{1}{1 + e^{-\frac{(20+V)}{12}}}$	S28
$\sigma_v = \frac{V_{cyt}}{V_{er}}$	S29
$\mathbf{J}_{mem} = -(\alpha I_{Ca} + k_{PMCA} Ca)$	S30
$\mathbf{J}_{er} = J_{leak} - J_{SERCA}$	S31
$\mathbf{J}_{leak} = p_{leak}(Ca_{er} - Ca)$	S32
$\mathbf{J}_{SERCA} = k_{SERCA} Ca$	S33
$FBP = 0.3\ G6P$	S34
$\mathbf{R}_{GPDH} = 0.2\sqrt{FBP}$	S35
$\gamma = \frac{v_\gamma R_{GPDH}}{k_\gamma + R_{GPDH}}$	S36

Where, C_m is the membrane capacitance, I_K is a V-dependent K^+ current, I_{Ca} is a V-dependent Ca^{2+} current, $I_{K(Ca)}$is a Ca^{2+}-activated K^+ current, and $I_{K(ATP)}$ is an ATP-sensitive K^+ current. τ_n is a time constant and n_∞ (V) is the equilibrium value of n as a function of V. The slow response of V is regulated by the gating variable 'n' that increases the conductance of the channel as V increases with time constant τ_n. O_∞ is a conductance function. g_k is the conductance of K^+ current and g_{Ca} (pS) is the conductance of Ca^{2+} current. $g_{K(Ca)}$ is the conductance of Ca^{2+} dependent K^+ current and $g_{K(ATP)}$ is the conductance of ATP regulated K^+ current.

Ca is the cytosolic Ca^{2+} concentration and Caer is the Ca^{2+} concentration in ER. f_{cyt} is the fraction of free to total cytosolic Ca^{2+}, f_{er} is the fraction of free to total ER Ca^{2+}, Jmem is the Ca^{2+} flux across the plasma membrane and J_{er} is the Ca^{2+}flux out of the endoplasmic

reticulum. α converts current to flux, and k_{PMCA} is the Ca^{2+} pump rate. J_{leak} is the Ca^{2+} flux out of the ER and J_{SERCA} is the Ca^{2+} flux into the ER through SERCA pumps. P_{leak} is the leakage permeability and k_{SERCA} is the SERCA pump rate.

G6P is Glucose 6-Phosphate concentration (in μM) and FBP is the Fructose-1,6-bisphosphate concentration (in μM). R_{GK} is the glucokinase reaction rate (in μM s^{-1}). R_{PFK} is the phosphofructokinase reaction rate (in μM s^{-1}). R_{GPDH} is the glyceraldehyde 3-P dehydrogenase reaction rate (in μM s^{-1}).

ADP is the Adenosine diphosphate concentration. γ is a function of ADP incorporated from glycolysis. v_γ and k_γ are constants. τ_a is a time constant. For further details consult the paper by Bertram et al..

Table – S3: Values of the parameters used for Module-1

$C_m = 5.3\times10^3$ fF	$g_K = 2.7\times10^3$ pS	$g_{Ca} = 1\times10^4$ pS
$g_{K(Ca)} = 6\times10^2$ pS	$\overline{g_K(ATP)} = 25$ nS	$f_{cyt} = 0.01$
$f_{er} = 0.01$	$\alpha = 4.5 \times 10^{-6}$ fA^{-1} μM ms^{-1}	$k_{PMCA} = 0.2$ ms^{-1}
$P_{leak} = 2\times10^{-4}$ ms^{-1}	$k_{SERCA} = 0.4$ ms^{-1}	$v_\gamma = 2.2$
$k_\gamma = 10$ μM s^{-1}	$\tau_a = 3\times10^5$ ms	r=1
$r_1 = 0.35$ μM	$V_k = -75$ mV	$V_{cyt}/V_{er} = 31$
$K_1 = 30$ μM	$K_2 = 1$ μM	$K_3 = 5\times10^4$ μM
$K_4 = 1\times10^3$ μM	$f_{amp} = 0.02$	$f_{mt} = 20$
$f_{fbp} = 0.2$	$f_{bt} = 20$	$f_{atp} = 20$
$K_{dd} = 17$ μM	$K_{tt} = 1$ μM	$K_{td} = 26$ μM
$K_D = 0.5$ mM	$\tau_n = 20$ ms	$V_{ca} = 25$ mV
$V_{max} = 1$ μM s^{-1}	λ = 0.06	$A_{tot} = 3\times10^3$ μM

Model-details (Module – 2, 3 and 4)

Description of Module -2

We have taken the module-1 from the well-established model of Bertram et al. and developed our model of glucose and insulin induced PIP_3 dynamics by systematically adding the other modules. Here we first describe the module-2.

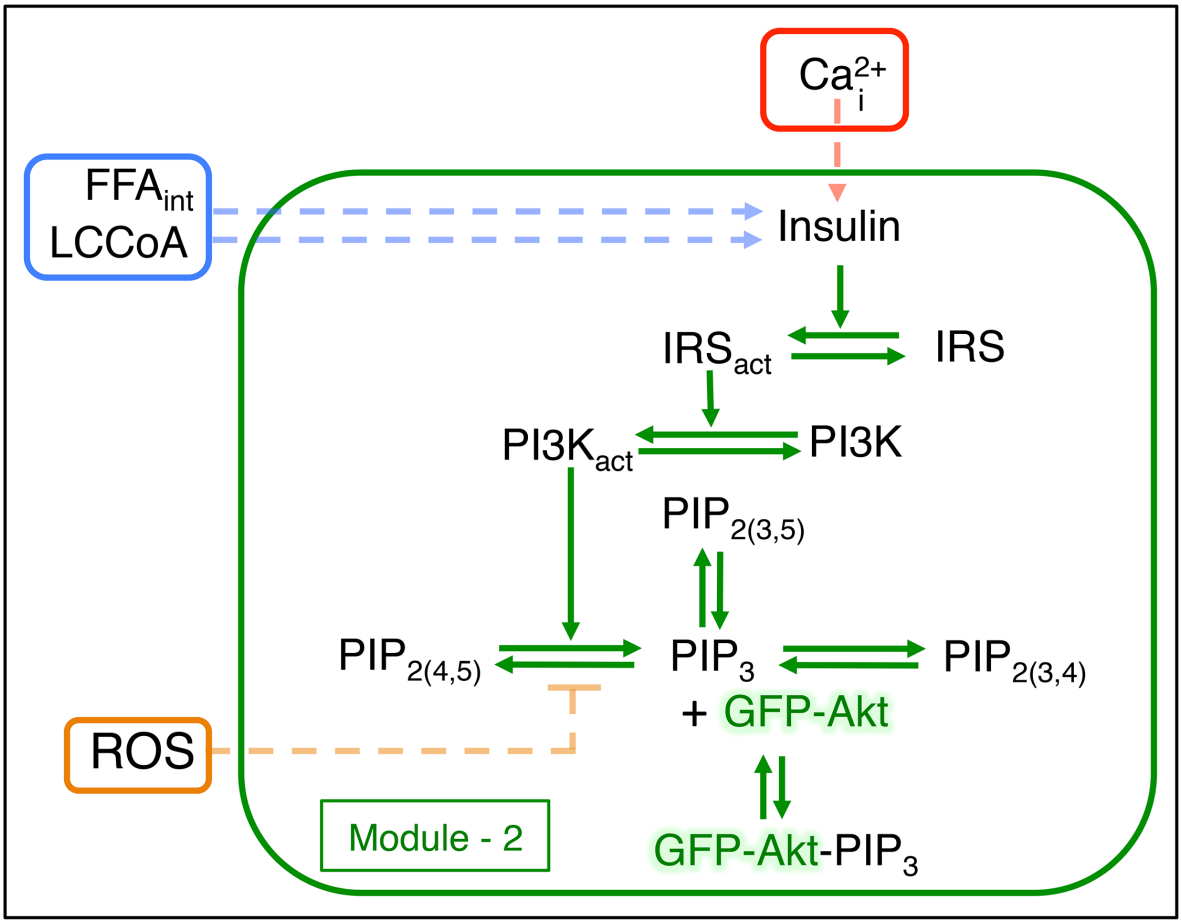

We start with describing the Eq.2 that phenomenologically depicts the dynamics of endogenous insulin in MIN6 β-cells. In the literature it is known that the cytosolic Ca^{2+} concentration critically controls the production of glucose induced endogenous insulin secretion and this regulation is extremely complex in nature.

$\frac{dI_{end}}{dt} = \frac{k_{Ifor} \times Ca^6}{k_{for}^6 + Ca^6} - k_{Icon} \times I_{end} + k_{Iccoa} \times LCCoA + k_{int} \times (FFA_{total} - FFA_{ex})$	2

To incorporate such a complex kind of regulation, we have used a Hill type of kinetics involving cytosolic Ca^{2+} concentration to represent the synthesis of endogenous insulin in MIN6 β-cells. The degradation of endogenous insulin protein is incorporated in the form of a first order kinetics in the subsequent term. In the literature there are evidences that glucose can activate the endogenous insulin independent of the Ca^{2+} signaling. In this regard, we have introduced two such effects in Eq.2. Externally added glucose can elevate the level of long chain acyl-CoA (LCCoA) through intracellular metabolism of free fatty acids (FFAs) that leads to the direct and even indirect (via generating complex lipids such as triglycerides (TG)) insulin secretion in β-cells. We have taken two simple first order terms (3rd and the 4th terms in Eq.2) to phenomenologically introduce the effect of other glucose induced Ca^{2+} signaling independent activation of insulin in β-cells.

The secreted insulin from MIN6 β-cells will eventually activate the insulin receptor substrate (IRS) protein. This has been modeled again in Eq.3 using phenomenological kinetic terms. In this case, we assume that the total concentration of IRS protein remains constant during the time frame of the experiments and further modeled the insulin dependent activation of IRS protein by a Hill type kinetic term.

$$\frac{\mathbf{dIRS_{act}}}{\mathbf{dt}} = \boldsymbol{k}_{\mathbf{for1}} \times (\mathbf{IRS_{total}} - \mathbf{IRS_{act}}) \times \frac{(\mathbf{I_{end}} + \mathbf{I_{ex}})^2}{\boldsymbol{k}_{\mathbf{mi}}^2 + (\mathbf{I_{end}} + \mathbf{I_{ex}})^2} - \boldsymbol{k}_{\mathbf{rev1}} \times \mathbf{IRS_{act}} \quad \mathbf{3}$$

To account for the experimental observation made by Hagren et al. we introduced the term (I_{ex}) in the Hill term, which essentially represents the amount of externally added insulin concentration during the experiments. Under normal condition I_{ex}=0. We further assumed that there is a steady deactivation rate of the activated IRS protein.

This insulin-induced activation of IRS protein ultimately leads to the activation of Phosphoinositide 3'-OH-kinase (PI3K).

The IRS_{act} mediated activation and subsequent deactivation of PI3K have been modeled with two simple mass-action kind of terms. Here again we assumed that the total protein concentration of the PI3K is constant.

$$\frac{\mathbf{dPI3K_{act}}}{\mathbf{dt}} = \boldsymbol{k}_{\mathbf{for2}} \times (\mathbf{PI3K_{total}} - \mathbf{PI3K_{act}}) \times \mathbf{IRS_{act}} - \boldsymbol{k}_{\mathbf{rev2}} \times \mathbf{PI3K_{act}} \quad (4)$$

Eq.5-8 forms the integral part of the module-2. Here we considered and modeled the detailed kinetic scheme of the Phosphatidylinositol phosphorylation dynamics, which initiates with the $PI3K_{act}$ mediated phosphorylation of Phosphatidylinositol (4,5)-bisphosphate ($PIP_{2(4,5)}$) to Phosphatidylinositol (3,4,5)-trisphosphate (PIP_3). This event has been modeled by the first term in the Eq.7 where we have also introduced the provision of including the effect of PI3K inhibitor LY294002 (Ly) by putting a phenomenological term in the denominator of the phosphorylation rate constant k_{for3}. Under normal condition Ly=0.

$$\frac{\boldsymbol{d}\mathbf{PIP35}}{\boldsymbol{dt}} = \boldsymbol{k}_{\mathbf{pip35}} \times \mathbf{PIP3} - \boldsymbol{k}_{\mathbf{dpip35}} \times \mathbf{PIP35} \quad (5)$$

$$\frac{\boldsymbol{d}\mathbf{PIP34}}{\boldsymbol{dt}} = \boldsymbol{k}_{\mathbf{pip34}} \times \mathbf{PIP3} - \boldsymbol{k}_{\mathbf{dpip34}} \times \mathbf{PIP34} \quad (6)$$

$$\begin{aligned}\frac{\mathbf{dPIP3}}{\mathbf{dt}} = {} & \frac{\boldsymbol{k}_{\mathbf{for3}}}{\mathbf{1} + \boldsymbol{k}_{\mathbf{for32}} \times \mathbf{Ly}} \times (\mathbf{PIP_{total}} - \mathbf{PIP35} - \mathbf{PIP34} - \mathbf{PIP3} - \mathbf{GFPAktPIP3}) \times \mathbf{PI3K_{act}} - \boldsymbol{k}_{\mathbf{pip35}} \times \mathbf{PIP3} \\ & + \boldsymbol{k}_{\mathbf{dpip35}} \times \mathbf{PIP35} - \boldsymbol{k}_{\mathbf{pip34}} \times \mathbf{PIP3} + \boldsymbol{k}_{\mathbf{dpip34}} \times \mathbf{PIP34} - \frac{\boldsymbol{k}_{\mathbf{rev3}}}{\mathbf{1} + \frac{\boldsymbol{k}_{\mathbf{r}}}{\mathbf{1} + \boldsymbol{k}_{\mathbf{for32}} \times \mathbf{Ly}} \times \mathbf{ROS}} \times \mathbf{PIP3} \\ & - \boldsymbol{k}_{\mathbf{for4}} \times (\mathbf{GFPAkt_{total}} - \mathbf{GFPAktPIP3}) \times \mathbf{PIP3} + \boldsymbol{k}_{\mathbf{rev4}} \times \mathbf{GFPAktPIP3}\end{aligned} \quad (7)$$

$$\frac{\mathbf{dGFPAktPIP3}}{\mathbf{dt}} = \boldsymbol{k}_{\mathbf{for4}} \times (\mathbf{GFPAkt_{total}} - \mathbf{GFPAktPIP3}) \times \mathbf{PIP3} - \boldsymbol{k}_{\mathbf{rev4}} \times \mathbf{GFPAktPIP3} \quad (8)$$

The dephosphorylation event of PIP_3 to $PIP_{2(4,5)}$ in this case is governed by PTEN, which we have modeled by k_{rev3}. PIP_3 term and we have further included two important effects in this regard: (i) Reactive oxygen species

(ROS) is well known to inhibit the effect of PTEN. That is why we have incorporated phenomenologically the ROS concentration to the denominator of k_{rev3}. (ii) The PI3K inhibitor, LY294002 (Ly) had also been shown to be an inhibitor of ROS. We have taken care of that effect as well in the same term of Eq.7. We have further assumed that PIP_3 can remain in phosphorylation-dephosphorylation equilibrium with either $PIP_{2(3,5)}$ (Eq.5) or $PIP_{2(3,4)}$ (Eq.6) and the total concentration of the PIP (PIP_{Total}) is considered to be constant as observed for few mammalian cells[1]. To reconcile the experimental results of Hagren et al. where they have seen a rise in the membrane localization of GFPAkt, we have introduced Eq.8. In this equation we have explicitly considered the complex formation between PIP_3 and GFPAkt and the corresponding decomplexation event. Again for the sake of simplicity we have considered that the total GFPAkt ($GFPAkt_{total}$) concentration remains constant during the course of the experiment.

Description of Module -3

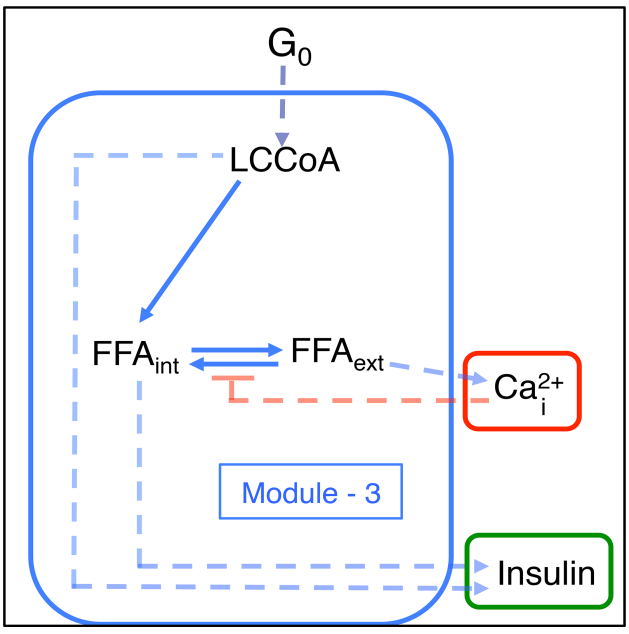

Hagren et al. observed experimentally that in absence of cytosolic Ca^{2+} signaling (i.e., in presence of diazoxide), the levels of secreted insulin from MIN6 β-cells at 3 mM and 20 mM glucose concentrations remain similar to

the insulin secreted in case of wild type situation with 3 mM glucose concentration. This clearly showed that there are alternative ways to activate endogeneous insulin secretion by adding glucose even in absence of cytosolic Ca^{2+} signaling. Free fatty acids (FFA) mediated regulatory pathways in more than one way activate the insulin secretion in β-cells. Externally added glucose can increase the level of long chain acyl-CoA (LCCoA) and this LCCoA can activate the insulin secretion through FFA dependent and independent mechanism. How these pathways exactly function is yet remain to be fully established experimentally, so we have again modeled this part phenomenologically. In Eq.9 we have assumed that the LCCoA production in β-cell depends on the external glucose concentration that follows a Hill type of kinetics to comply with the observations made by Hagren et al.. We have further modeled the degradation rate of LCCoA as simple first order kinetics.

$\frac{\mathbf{dLCCoA}}{\mathbf{dt}} = \boldsymbol{k}_{\mathbf{factor}} \times \frac{\boldsymbol{G}_0^2}{\boldsymbol{G}_0^2 + \boldsymbol{k}_i^2} - \boldsymbol{k}_{\mathbf{dis1}} \times \mathbf{LCCoA}$	9
$\frac{\mathbf{dFFA_{ex}}}{\mathbf{dt}} = \boldsymbol{k}_{\mathbf{a}} \times \mathbf{LCCoA} \times (\mathbf{FFA_{total}} - \mathbf{FFA_{ex}}) - \left(\frac{\boldsymbol{k}_{\mathbf{b}}}{\mathbf{1} + (\boldsymbol{k}_{\mathbf{c}} \times \mathbf{Ca})}\right) \times \mathbf{FFA_{ex}}$	10

On the other hand, it is known in the literature that externally added glucose can regulate the Triglyceride (TG)/FFA cycling and in turn renew the intracellular FFA (FFA_{int}) to a certain level in a LCCoA dependent manner. A portion of the intracellular FFA crosses the cell membrane and act simultaneously with extracellular FFA (FFA_{ext}) to activate the G-protein coupled free fatty acid receptor (GPR40/FEAR)[2,3] that in turn results in the enhancement of the insulin secretion in β-cell. We have modeled the glucose mediated regulation of insulin secretion through intracellular FFA dynamics in an over simplified way by introducing Eq.10 and putting the effect of FFA_{int} in Eq.2. In Eq.10 we assume that LCCoA and cytosolic Ca^{2+} concentrations tightly control the level of intracellular FFA in order to reproduce the experimental observation made by Hagren et al..

Description of Module -4

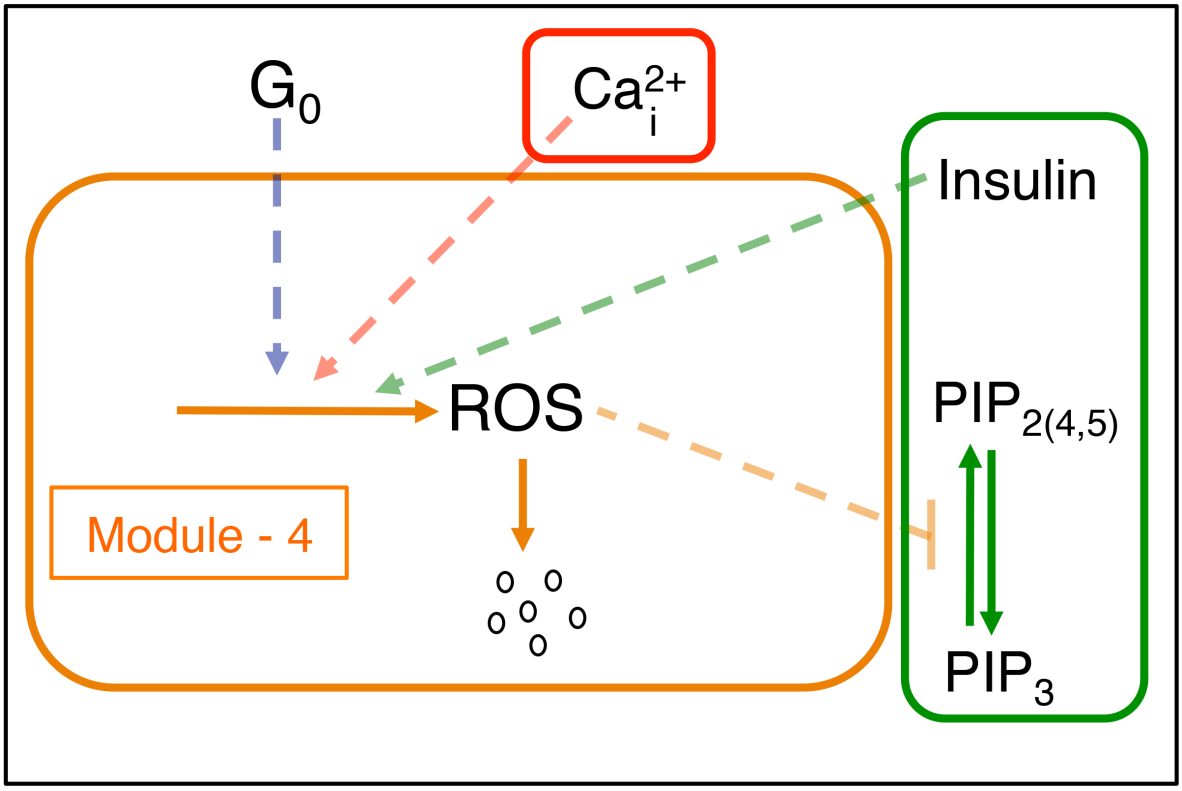

One of the crucial finding made by the Hagren et al. was to show that both glucose and insulin synergistically control the PIP_3 dynamics in the β-cell membrane. They showed that even in absence of Ca^{2+} signaling and at high external concentration of insulin, adding glucose externally could alter the PIP3 dynamics in a dose dependent manner. Hagren et al. did not provide any specific reason for such observation but speculated that ROS signaling might be responsible for it. We searched through the literature and figured out that ROS signaling could in principle cause such an abrupt rise in PIP_3 dynamics and we modeled again in a phenomenological manner.

$$\frac{\mathbf{dROS}}{\mathbf{dt}} = \frac{k_{\mathrm{rca}} \times \mathrm{Ca}}{1 + k_{\mathrm{ca}} \times \mathrm{Ca}^2} + \frac{k_{\mathrm{ros}} \times G_0^2 \times (\mathrm{I_{end}} + \mathrm{I_{ex}})^2}{k_m^2 + (\mathrm{I_{end}} + \mathrm{I_{ex}})^2} - k_{\mathrm{dros}} \times \mathrm{ROS} \qquad (11)$$

Eq.11 depicts how we have included the effect of ROS activity in MIN6 β-cell in a phenomenological manner. Intracellular Ca^{2+} is known to induce the ROS

productions in more than one way in mammalian cells but if required it can even activate the antioxidant defense mechanism to protect cells from higher levels of ROS[4]. We have modeled this overall Ca^{2+} dependent ROS activation by the 1st term given in Eq.11 where for lower concentration of Ca^{2+} will initially increase ROS level but as the cytosolic Ca^{2+} becomes very high then it will eventually decrease the ROS production as observed experimentally. The 2nd term in Eq.11 takes care of the fact that in insulin resistant cells the ROS generation is dependent heavily on the pathways such as auto oxidation of glucose[5] and advanced glycation end product[6] mediated signaling. It has also been found that insulin itself can activate the ROS generation. We have modeled all these biological observations again phenomenologically. The 2nd term in Eq.11 essentially suggests if either the level of endogenously secreted insulin or externally added insulin are very high, then only the ROS generation will be highly dependent on external glucose concentration. That is the pathways related to auto oxidation of glucose[5] and advanced glycation end product[6] mediated signaling will get activated in a situation where the cells are experiencing an insulin saturated or perhaps an insulin resistant state. We further modeled the ROS degradation as simple first order degradation kinetics. We have already discussed how the activated ROS can regulate the PIP_3 dynamics by inhibiting the phosphatase PTEN and that we have taken into account in Eq.7.

Reference

1 S. McLaughlin, J. Wang, A. Gambhir and D. Murray, *Annu. Rev. Biophys. Biomol. Struct.*, 2002, **31**, 151–175.

2 C. J. Nolan, M. S. R. Madiraju, V. Delghingaro-Augusto, M.-L. Peyot and M. Prentki, *Diabetes*, 2006, **55**, S16–S23.

3 C. P. Briscoe, M. Tadayyon, J. L. Andrews, W. G. Benson, J. K. Chambers, M. M. Eilert, C. Ellis, N. A. Elshourbagy, A. S. Goetz, D. T. Minnick, P. R. Murdock, H. R. Sauls, U. Shabon, L. D. Spinage, J. C. Strum, P. G. Szekeres, K. B. Tan, J. M. Way, D. M. Ignar, S. Wilson and A. I. Muir, *J. Biol. Chem.*, 2003, **278**, 11303–11311.

4 Y. Yan, C. L. Wei, W. R. Zhang, H. P. Cheng and J. Liu, *Acta Pharmacol. Sin.*, 2006, **27**, 821–826.

5 J. V. Hunt, C. C. T. Smith and S. P. Wolff, *Diabetes*, 1990, **39**, 1420–1424.

6 J. V Hunt, M. a Bottoms and M. J. Mitchinson, *Biochem. J.*, 1993, **291**, 529–535.

7 J. C. Henquin, D. Dufrane and M. Nenquin, *Diabetes*, 2006, **55**, 3470–3477.

8 J. S. Dillon, G. C. Yaney, Y. Zhou, N. Voilley, S. Bowen, S. Chipkin, C. R. Bliss, V. Schultz, F. C. Schuit, M. Prentki, D. J. Waxman and B. E. Corkey, *Diabetes*, 2000, **49**, 2010-2020.

Supplementary Figures

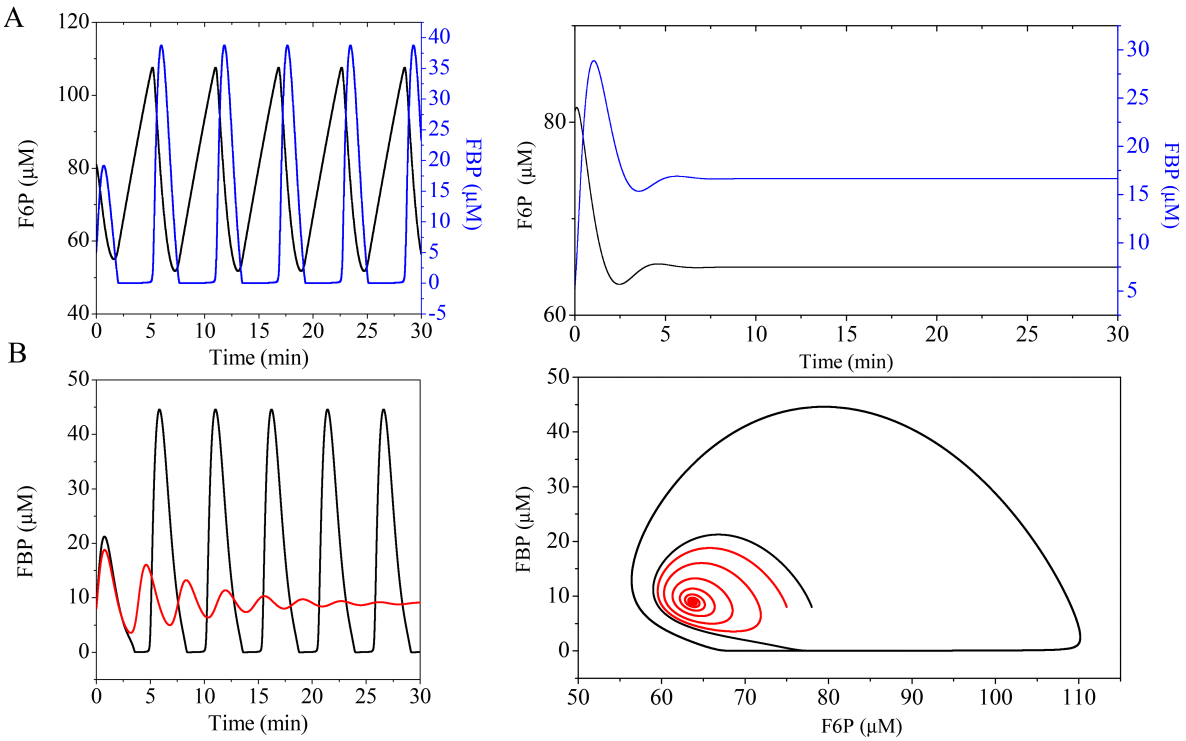

Figure S1: The oscillation and bistability of glycolytic subsystem. (A) Oscillations in glycolytic components (FBP and F6P) in presence of 11 mM glucose (left). The glycolytic oscillation for the glycolytic components approach steady states for 20 mM glucose (right). (B) The FBP concentration variation with time for different concentrations of F6P (75 μM for red and 78 μM for black curves respectively) (left). The glycolytic subsystem shows a bistable behavior (right) for 16 mM glucose concentration. With 75 μM of initial condition of F6P, the trajectory spirals (red) into a steady state and as the initial condition of F6P changed to 78 μM, it produces a stable steady oscillation (black).

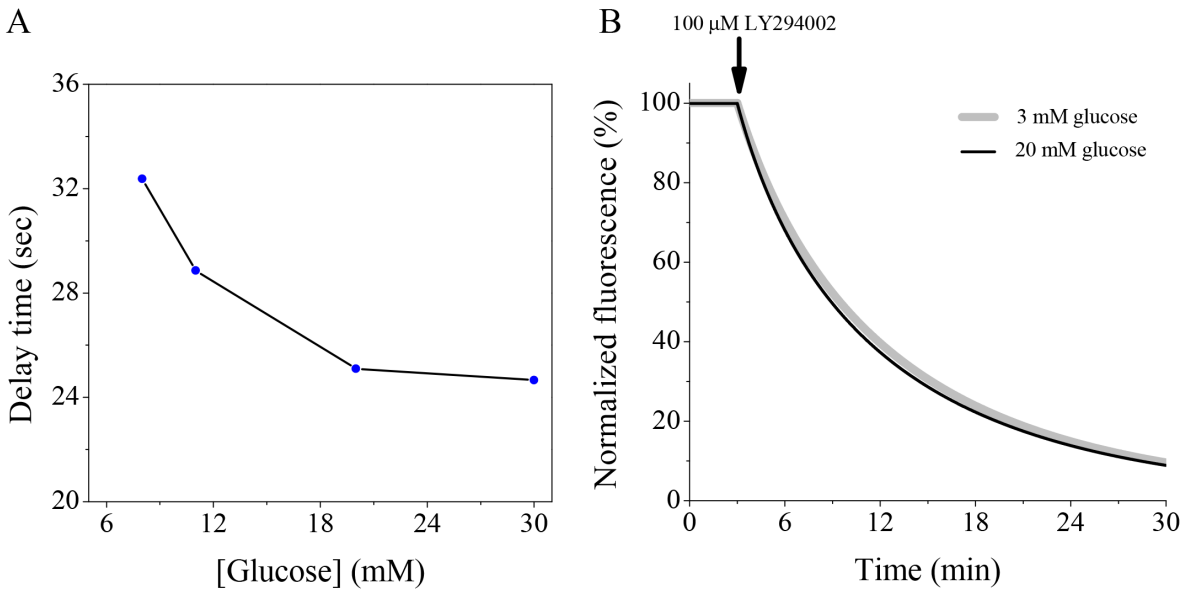

Figure S2: (A) The exponential decrease in the time delay of GFP-PH_{Akt} translocation as the glucose concentration is elevated from 3 mM to higher concentrations in presence of 100 nM external insulin and 250 µM of diazoxide. (B) Effect of PI3-kinase inhibitor (LY294002) in insulin induced GFP-PH_{Akt} translocation. In presence of LY294002, insulin induced GFPAkt translocation reverses to the base value in a similar manner for 3 mM as well as 20 mM glucose concentrations.

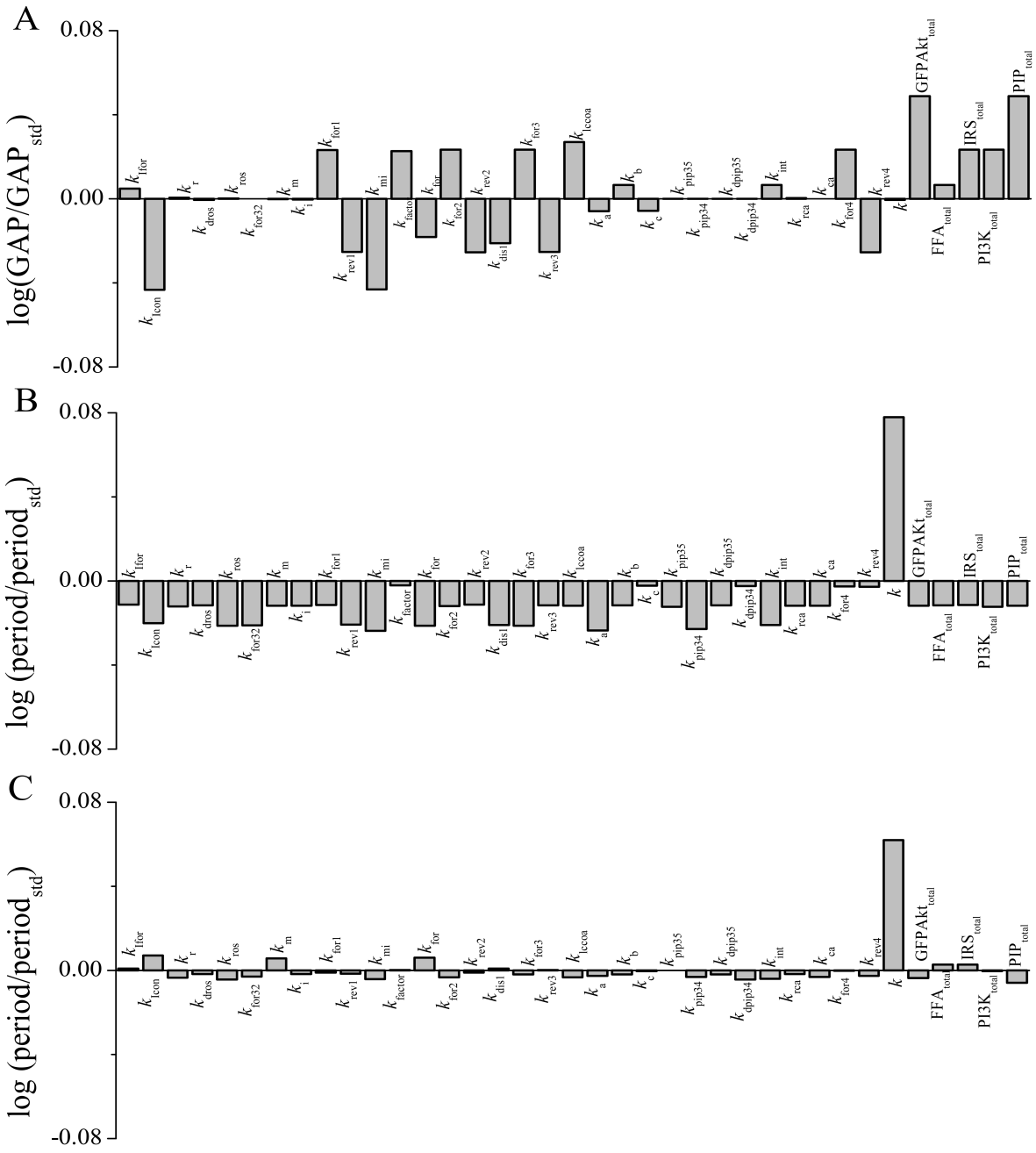

Figure S3: Sensitivity analysis of the parameters involved in the model. In all the cases, parameters are increased individually (about 20% of the values provided in the Table-3, main text) keeping all other parameters constant. **(A)** The change in the GFP-PH_{Akt} translocation is measured on the basis of change in the GFP-PH_{Akt} translocation observed with respect to the standard GFP-PH_{Akt} translocation at 3 mM glucose concentration. **(B)** The sensitivity is measured by measuring the changes in the oscillation period as one of the parameter is increased individually about 20% of its original value (provided in Table-3), and the oscillation period is compared with respect to the standard oscillation period at 11 mM glucose concentration. **(C)** The sensitivity is measured by measuring the changes in the oscillation period as one of the parameter is increased individually about 20% of its original value (provided in Table-3), and the oscillation period is compared with respect to the standard oscillation period at 20 mM glucose concentration.

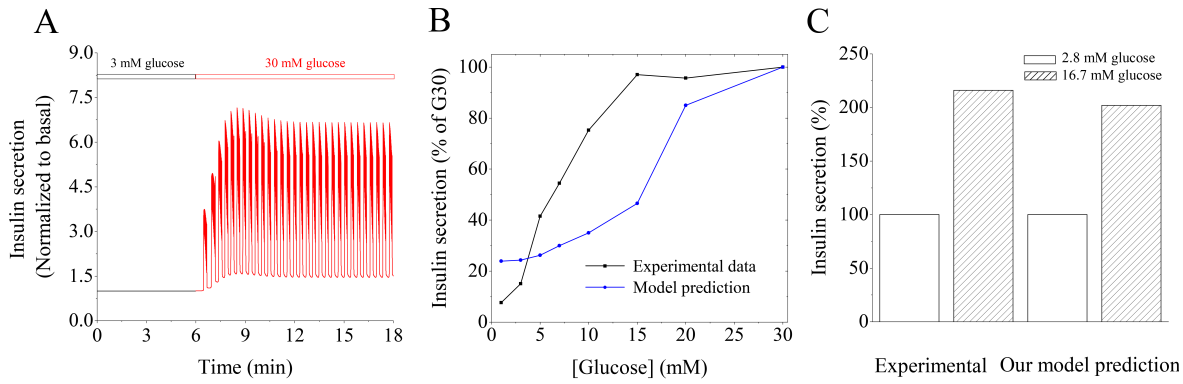

Figure S4: (A) The increase in the insulin secretion amount (Normalized to the basal level) in the MIN6 β-cells as the external glucose level is increased from 3 mM (black line) to 30 mM (red line). **(B)** The effect of externally added glucose concentration on insulin secretion in normal human islets (black line, experiment[7]) and blue line (model prediction). **(C)** The relative increase in the secreted insulin level for 2.8 and 16.7 mM glucose concentration in the rodent pancreatic β- cells. Numerically, the insulin level at 16.7 mM glucose concentration is measured by normalizing it with respect to the basal insulin level (assuming at 2.8 mM glucose concentration the insulin secretion is 100%) as followed in the experiment[8].